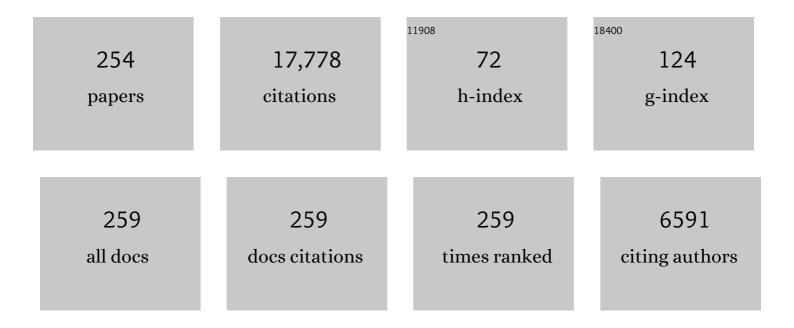
Yi-Gang Xu

List of Publications by Year in descending order

Source: https://exaly.com/author-pdf/6956159/publications.pdf Version: 2024-02-01



YI-GANG XII

#	Article	IF	CITATIONS
1	Cretaceous basin evolution in northeast Asia: tectonic responses to the paleo-Pacific plate subduction. National Science Review, 2022, 9, nwab088.	4.6	33
2	Constraining the duration of the Tarim flood basalts (northwestern China): CA-TIMS zircon U-Pb dating of tuffs. Bulletin of the Geological Society of America, 2022, 134, 325-334.	1.6	10
3	Raman spectroscopy-based screening of zircon for reliable water content and oxygen isotope measurements. American Mineralogist, 2022, 107, 936-945.	0.9	5
4	Improved age estimates for Holocene Ko-g and Ma-f~j tephras in northern Japan using Bayesian statistical modelling. Quaternary Geochronology, 2022, 67, 101229.	0.6	4
5	Mid-Cretaceous Wake seamounts in NW Pacific originate from secondary mantle plumes with Arago hotspot composition. Chemical Geology, 2022, 587, 120632.	1.4	13
6	Molybdenum isotopic constraints on the origin of EM1-type continental intraplate basalts. Geochimica Et Cosmochimica Acta, 2022, 317, 255-268.	1.6	13
7	Azimuthal Anisotropy Tomography of the Southeast Asia Subduction System. Journal of Geophysical Research: Solid Earth, 2022, 127, .	1.4	29
8	Holocene Tephrostratigraphy in the East Sea/Japan Sea: Implications for Eruptive History of Ulleungdo Volcano and Potential for Hemispheric Synchronization of Sedimentary Archives. Journal of Geophysical Research: Solid Earth, 2022, 127, .	1.4	3
9	Boron isotopes in boninites document rapid changes in slab inputs during subduction initiation. Nature Communications, 2022, 13, 993.	5.8	17
10	Anisotropic Tomography and Dynamics of the Big Mantle Wedge. Geophysical Research Letters, 2022, 49, .	1.5	21
11	Co-Occurrence of HIMU and EM1 Components in a Single Magellan Seamount: Implications for the Formation of West Pacific Seamount Province. Journal of Petrology, 2022, 63, .	1.1	4
12	High Water Contents in Zircons Suggest Waterâ€Fluxed Crustal Melting During Cratonic Destruction. Geophysical Research Letters, 2022, 49, .	1.5	1
13	Exploring small-scale recycled mantle components with intraplate continental twin volcanoes. Chemical Geology, 2022, 598, 120842.	1.4	1
14	Migration of Middle-Late Jurassic volcanism across the northern North China Craton in response to subduction of Paleo-Pacific Plate. Tectonophysics, 2022, 833, 229338.	0.9	6
15	Thermal and compositional anomalies in a detailed xenolith-based lithospheric mantle profile of the Siberian craton and the origin of seismic midlithosphere discontinuities. Geology, 2022, 50, 891-896.	2.0	18
16	Pn Anisotropic Tomography of Hainan Island and Surrounding Areas: New Insights Into the Hainan Mantle Plume. Journal of Geophysical Research: Solid Earth, 2022, 127, .	1.4	7
17	Magmatic perspective on subduction of Paleo-Pacific plate and initiation of big mantle wedge in East Asia. Earth-Science Reviews, 2021, 213, 103473.	4.0	89
18	Mercury fluxes record regional volcanism in the South China craton prior to the end-Permian mass extinction. Geology, 2021, 49, 452-456.	2.0	57

#	Article	IF	CITATIONS
19	Optimization of irradiation parameters for 40Ar/39Ar dating by Argus VI multi-collector mass spectrometry. Journal of Analytical Atomic Spectrometry, 2021, 36, 1374-1380.	1.6	6
20	Permian ridge subduction in the easternmost Central Asian Orogenic Belt: Magmatic record using Sr-Nd-Pb-Hf-Mg isotopes. Lithos, 2021, 384-385, 105966.	0.6	7
21	Mesozoic intraplate tectonism of East Asia due to flat subduction of a composite terrane slab. Earth-Science Reviews, 2021, 214, 103505.	4.0	39
22	Lateral Seismic Anisotropy Variations Record Interaction Between Tibetan Mantle Flow and Plume‧trengthened Yangtze Craton. Journal of Geophysical Research: Solid Earth, 2021, 126, e2020JB020841.	1.4	17
23	High-precision geochronological constraints on the duration of â€~Dinosaur Pompeii' and the Yixian Formation. National Science Review, 2021, 8, nwab063.	4.6	34
24	Origin of Graphite–Diamond-Bearing Eclogites from Udachnaya Kimberlite Pipe. Journal of Petrology, 2021, 62, .	1.1	8
25	Metamorphic <i>P</i> – <i>T</i> – <i>t</i> – <i>d</i> evolution of the Mesoproterozoic Purâ€Banera supracrustal belt, Aravalli Craton, northwestern India: Insights from phase equilibria modelling and zircon–monazite geochronology of metapelites. Journal of Metamorphic Geology, 2021, 39, 1173-1204.	1.6	9
26	Nature of the Mantle Plume Under the Emeishan Large Igneous Province: Constraints From Olivineâ€Hosted Melt Inclusions of the Lijiang Picrites. Journal of Geophysical Research: Solid Earth, 2021, 126, e2020JB021022.	1.4	11
27	Cryptic zoning in primitive olivine as an archive of mush fluidization at mid-ocean ridges. Lithos, 2021, 390-391, 106121.	0.6	0
28	Dynamic processes of the curved subduction system in Southeast Asia: A review and future perspective. Earth-Science Reviews, 2021, 217, 103647.	4.0	39
29	Origin of potassic postcollisional volcanic rocks in young, shallow, blueschist-rich lithosphere. Science Advances, 2021, 7, .	4.7	7
30	Intermittent Postâ€Paleocene Continental Collision in South Asia. Geophysical Research Letters, 2021, 48, e2021GL094531.	1.5	4
31	Crustal SiO ₂ Content of the Emeishan Large Igneous Province and its Implications for Magma Volume and Plumbing System. Geochemistry, Geophysics, Geosystems, 2021, 22, e2021GC009783.	1.0	11
32	Short duration of Early Permian Qiangtang-Panjal large igneous province: Implications for origin of the Neo-Tethys Ocean. Earth and Planetary Science Letters, 2021, 568, 117054.	1.8	39
33	Magnesium isotope constraints on contributions of recycled oceanic crust and lithospheric mantle to generation of intraplate basalts in a big mantle wedge. Lithos, 2021, 398-399, 106327.	0.6	2
34	Evidence of Volatileâ€Induced Melting in the Northeast Asian Upper Mantle. Journal of Geophysical Research: Solid Earth, 2021, 126, e2021JB022167.	1.4	3
35	Formation mechanism of the North–South Gravity Lineament in eastern China. Tectonophysics, 2021, 818, 229074.	0.9	12
36	Geochronology, petrology, and lithium isotope geochemistry of the Bailongshan granite-pegmatite system, northern Tibet: Implications for the ore-forming potential of pegmatites. Chemical Geology, 2021, 584, 120484.	1.4	20

#	Article	IF	CITATIONS
37	Olivine chemistry of the Quaternary Datong basalts of the Trans-North China Orogen: insights into mantle source lithology and redox–hydration state. Geological Society Special Publication, 2021, 510, 115-131.	0.8	2
38	Molybdenum isotopes unmask slab dehydration and melting beneath the Mariana arc. Nature Communications, 2021, 12, 6015.	5.8	23
39	Felsic volcanism as a factor driving the end-Permian mass extinction. Science Advances, 2021, 7, eabh1390.	4.7	63
40	Eoarchean to Paleoproterozoic crustal evolution in the North China Craton: Evidence from U-Pb and Hf-O isotopes of zircons from deep-crustal xenoliths. Geochimica Et Cosmochimica Acta, 2020, 278, 94-109.	1.6	49
41	Mineralogical constraints on the magmatic–hydrothermal evolution of rare-elements deposits in the Bailongshan granitic pegmatites, Xinjiang, NW China. Lithos, 2020, 352-353, 105208.	0.6	20
42	Oxidized Late Mesozoic subcontinental lithospheric mantle beneath the eastern North China Craton: A clue to understanding cratonic destruction. Gondwana Research, 2020, 81, 230-239.	3.0	19
43	Lithium isotope fractionation during fluid exsolution: Implications for Li mineralization of the Bailongshan pegmatites in the West Kunlun, NW Tibet. Lithos, 2020, 352-353, 105236.	0.6	30
44	Stability and migration of slab-derived carbonate-rich melts above the transition zone. Earth and Planetary Science Letters, 2020, 531, 116000.	1.8	15
45	Calcium isotopic composition of the lunar crust, mantle, and bulk silicate Moon: A preliminary study. Geochimica Et Cosmochimica Acta, 2020, 270, 313-324.	1.6	14
46	Western Northern Luzon Isotopic Evidence of Transition From Proto outh China Sea to South China Sea Fossil Ridge Subduction. Tectonics, 2020, 39, e2019TC005639.	1.3	15
47	Partial Melting of the Lower Oceanic Crust: Implications for Tracing the Slab Component in the Source of Midâ€Ocean Ridge Basalts. Journal of Geophysical Research: Solid Earth, 2020, 125, e2020JB020673.	1.4	2
48	Holocene tephrostratigraphic framework and monsoon evolution of East Asia: Key tephra beds for synchronising palaeoclimate records. Quaternary Science Reviews, 2020, 242, 106467.	1.4	7
49	Neoarchaean crustal reworking in the Aravalli Craton: Petrogenesis and tectonometamorphic history of the Malola granite, Bhilwara area, northwestern India. Geological Journal, 2020, 55, 8186-8210.	0.6	8
50	The origin of arc basalts: New advances and remaining questions. Science China Earth Sciences, 2020, 63, 1969-1991.	2.3	21
51	Oxidation State of the Lithospheric Mantle Beneath Komsomolskaya–Magnitnaya Kimberlite Pipe, Upper Muna Field, Siberian Craton. Minerals (Basel, Switzerland), 2020, 10, 740.	0.8	6
52	The age and origin of cratonic lithospheric mantle: Archean dunites vs. Paleoproterozoic harzburgites from the Udachnaya kimberlite, Siberian craton. Geochimica Et Cosmochimica Acta, 2020, 281, 67-90.	1.6	22
53	Geochronology and geochemistry of the fossil-flora-bearing Wuda Tuff in North China Craton and its tectonic implications. Lithos, 2020, 364-365, 105485.	0.6	11
54	Anatexis and metamorphic history of Permian pelitic granulites from the southern Chinese Altai: Constraints from petrology, melt inclusions and phase equilibria modelling. Lithos, 2020, 360-361, 105432.	0.6	6

#	Article	IF	CITATIONS
55	Geology and geochronology of the super-large Bailongshan Li–Rb–(Be) rare-metal pegmatite deposit, West Kunlun orogenic belt, NW China. Lithos, 2020, 360-361, 105449.	0.6	32
56	Geochemical, biostratigraphic, and high-resolution geochronological constraints on the waning stage of Emeishan Large Igneous Province. Bulletin of the Geological Society of America, 2020, 132, 1969-1986.	1.6	39
57	Recycled carbonate-induced oxidization of the convective mantle beneath Jiaodong, Eastern China. Lithos, 2020, 366-367, 105544.	0.6	11
58	The Mantle Transition Zone Hosts the Missing HIMU Reservoir Beneath Eastern China. Geophysical Research Letters, 2020, 47, e2020GL087260.	1.5	6
59	Abrupt warming in the latest Permian detected using high-resolution in situ oxygen isotopes of conodont apatite from Abadeh, central Iran. Palaeogeography, Palaeoclimatology, Palaeoecology, 2020, 560, 109973.	1.0	35
60	<italic>Destruction of the North China Craton</italic> : Multidisciplinary efforts over past ten years. Chinese Science Bulletin, 2020, 65, 3860-3861.	0.4	0
61	Zircon U-Pb age and Hf-O isotope insights into genesis of Permian Tarim felsic rocks, NW China: Implications for crustal melting in response to a mantle plume. Gondwana Research, 2019, 76, 290-302.	3.0	9
62	Geochemical characterization of a reconstructed 1110â€ [−] Ma Large Igneous Province. Precambrian Research, 2019, 332, 105382.	1.2	37
63	Reply to comment by Qi and Wang on "Similar crust beneath disrupted and intact cratons: Arguments against lower-crust delamination as a decratonization trigger― Tectonophysics, 2019, 767, 128156.	0.9	0
64	Evidence of Early Cretaceous lower arc crust delamination and its role in the opening of the South China Sea. Gondwana Research, 2019, 76, 123-145.	3.0	17
65	Mesoarchaean to Neoproterozoic (3.2–0.8â€ ⁻ Ca) crustal growth and reworking in the Aravalli Craton, northwestern India: Insights from the Pur-Banera supracrustal belt. Precambrian Research, 2019, 332, 105383.	1.2	25
66	Mantle upwelling beneath the South China Sea and links to surrounding subduction systems. National Science Review, 2019, 6, 877-881.	4.6	26
67	The origins of high-Ti and low-Ti magmas in large igneous provinces, insights from melt inclusion trace elements and Sr-Pb isotopes in the Emeishan large Igneous Province. Lithos, 2019, 344-345, 122-133.	0.6	29
68	Oldest high-Ti basalt and magnesian crustal materials in feldspathic lunar meteorite Dhofar 1428. Geochimica Et Cosmochimica Acta, 2019, 266, 74-108.	1.6	7
69	Developing a Holocene tephrostratigraphy for northern Japan using the sedimentary record from Lake Kushu, Rebun Island. Quaternary Science Reviews, 2019, 215, 272-292.	1.4	13
70	Two distinct mantle convection systems and reservoirs in the West Pacific. Acta Geologica Sinica, 2019, 93, 31-31.	0.8	0
71	Establishing the link between Permian volcanism and biodiversity changes: Insights from geochemical proxies. Gondwana Research, 2019, 75, 68-96.	3.0	57
72	Molybdenum and boron isotope evidence for fluid-fluxed melting of intraplate upper mantle beneath the eastern North China Craton. Earth and Planetary Science Letters, 2019, 520, 105-114.	1.8	32

#	Article	IF	CITATIONS
73	The subduction of the west Pacific plate and the destruction of the North China Craton. Science China Earth Sciences, 2019, 62, 1340-1350.	2.3	219
74	Post-250†Ma thermal evolution of the central Cathaysia Block (SE China) in response to flat-slab subduction at the proto-Western Pacific margin. Gondwana Research, 2019, 75, 1-15.	3.0	22
75	Magmatic Processes Associated with Oceanic Crustal Accretion at Slow-spreading Ridges: Evidence from Plagioclase in Mid-ocean Ridge Basalts from the South China Sea. Journal of Petrology, 2019, 60, 1135-1162.	1.1	16
76	Is there a big mantle wedge under eastern Tibet?. Physics of the Earth and Planetary Interiors, 2019, 292, 100-113.	0.7	62
77	Development of a Dense Cratonic Keel Prior to the Destruction of the North China Craton: Constraints From Sedimentary Records and Numerical Simulation. Journal of Geophysical Research: Solid Earth, 2019, 124, 13192-13206.	1.4	11
78	Destruction of the North China Craton in the Mesozoic. Annual Review of Earth and Planetary Sciences, 2019, 47, 173-195.	4.6	428
79	High-precision measurement of B isotopes on low-boron oceanic volcanic rock samples via MC-ICPMS: Evaluating acid leaching effects on boron isotope compositions, and B isotopic variability in depleted oceanic basalts. Chemical Geology, 2019, 505, 76-85.	1.4	13
80	Crustal melting above a mantle plume: Insights from the Permian Tarim Large Igneous Province, NW China. Lithos, 2019, 326-327, 370-383.	0.6	17
81	Plume-ridge interaction in the South China Sea: Thermometric evidence from Hole U1431E of IODP Expedition 349. Lithos, 2019, 324-325, 466-478.	0.6	35
82	Similar crust beneath disrupted and intact cratons: Arguments against lower-crust delamination as a decratonization trigger. Tectonophysics, 2019, 750, 1-8.	0.9	14
83	Evaluating the effect of leaching on trace element and Nd-Pb isotopic systematics in continental basalts. Solid Earth Sciences, 2019, 4, 1-11.	0.8	1
84	Crustal Footprint of the Hainan Plume Beneath Southeast China. Journal of Geophysical Research: Solid Earth, 2018, 123, 3065-3079.	1.4	28
85	40Ar/39Ar dating of oceanic plagiogranite: Constraints on the initiation of seafloor spreading in the South China Sea. Lithos, 2018, 302-303, 421-426.	0.6	13
86	The influence of the double spike proportion effect on stable isotope (Zn, Mo, Cd, and Sn) measurements by multicollector-inductively coupled plasma-mass spectrometry (MC-ICP-MS). Journal of Analytical Atomic Spectrometry, 2018, 33, 555-562.	1.6	19
87	Reworking of Archean mantle in the NE Siberian craton by carbonatite and silicate melt metasomatism: Evidence from a carbonate-bearing, dunite-to-websterite xenolith suite from the Obnazhennaya kimberlite. Geochimica Et Cosmochimica Acta, 2018, 224, 132-153.	1.6	58
88	Subaqueous volcanism in the Paleo-Pacific Ocean based on Jurassic basaltic tuff and pillow basalt in the Raohe Complex, NE China. Science China Earth Sciences, 2018, 61, 1042-1056.	2.3	9
89	Melt Diversity and Magmatic Evolution in the Dali Picrites, Emeishan Large Igneous Province. Journal of Geophysical Research: Solid Earth, 2018, 123, 9635-9657.	1.4	10
90	Continental Arc and Backâ€Arc Migration in Eastern NE China: New Constraints on Cretaceous Paleoâ€Pacific Subduction and Rollback. Tectonics, 2018, 37, 3893-3915.	1.3	41

#	Article	IF	CITATIONS
91	An evaluation of precision and accuracy of SIMS oxygen isotope analysis. Solid Earth Sciences, 2018, 3, 81-86.	0.8	61
92	Craton Destruction 2: Evolution of Cratonic Lithosphere After a Rapid Keel Delamination Event. Journal of Geophysical Research: Solid Earth, 2018, 123, 10,069.	1.4	12
93	Generation of Cenozoic intraplate basalts in the big mantle wedge under eastern Asia. Science China Earth Sciences, 2018, 61, 869-886.	2.3	99
94	Craton Destruction 1: Cratonic Keel Delamination Along a Weak Midlithospheric Discontinuity Layer. Journal of Geophysical Research: Solid Earth, 2018, 123, 10,040.	1.4	24
95	Late Cenozoic basaltic lavas from the Changbaishan-Baoqing Volcanic Belt, NE China: Products of lithosphere-asthenosphere interaction induced by subduction of the Pacific plate. Journal of Asian Earth Sciences, 2018, 164, 260-273.	1.0	16
96	The provenance of late Permian karstic bauxite deposits in SW China, constrained by the geochemistry of interbedded clastic rocks, and U–Pb–Hf–O isotopes of detrital zircons. Lithos, 2017, 278-281, 240-254.	0.6	53
97	Thermochronological record of Middle–Late Jurassic magmatic reheating to Eocene rift-related rapid cooling in the SE South China Block. Gondwana Research, 2017, 46, 191-203.	3.0	24
98	Short episodes of crust generation during protracted accretionary processes: Evidence from Central Asian Orogenic Belt, NW China. Earth and Planetary Science Letters, 2017, 464, 142-154.	1.8	98
99	Hydrous orthopyroxene-rich pyroxenite source of the Xinkailing high magnesium andesites, Western Liaoning: Implications for the subduction-modified lithospheric mantle and the destruction mechanism of the North China Craton. Lithos, 2017, 282-283, 10-22.	0.6	18
100	Early Jurassic calc-alkaline magmatism in northeast China: Magmatic response to subduction of the Paleo-Pacific Plate beneath the Eurasian continent. Journal of Asian Earth Sciences, 2017, 143, 249-268.	1.0	60
101	Ultramafic to mafic granulites from the Larsemann Hills, East Antarctica: Geochemistry and tectonic implications. Journal of Asian Earth Sciences, 2017, 145, 679-690.	1.0	13
102	Differential partial melting process for temporal variations of Shandong basalts revealed by melt inclusions and their host olivines. Gondwana Research, 2017, 49, 205-221.	3.0	8
103	Phanerozoic magma underplating and crustal growth beneath the North China Craton. Terra Nova, 2017, 29, 211-217.	0.9	11
104	Primary magmas and mantle sources of Emeishan basalts constrained from major element, trace element and Pb isotope compositions of olivine-hosted melt inclusions. Geochimica Et Cosmochimica Acta, 2017, 208, 63-85.	1.6	68
105	Evolution of the mantle beneath the eastern North China Craton during the Cenozoic: Linking geochemical and geophysical observations. Journal of Geophysical Research: Solid Earth, 2017, 122, 224-246.	1.4	23
106	Unusually thickened crust beneath the Emeishan large igneous province detected by virtual deep seismic sounding. Tectonophysics, 2017, 721, 387-394.	0.9	12
107	Development of CA-ID-TIMS zircon U–Pb dating technique at Guangzhou Institute of Geochemistry, Chinese Academy of Sciences. Solid Earth Sciences, 2017, 2, 55-61.	0.8	2
108	Triggers on sulfide saturation in Fe–Ti oxide-bearing, mafic-ultramafic layered intrusions in the Tarim large igneous province, NW China. Mineralium Deposita, 2017, 52, 471-494.	1.7	5

#	Article	IF	CITATIONS
109	Sr-Nd-Pb isotopic compositions of the lower crust beneath northern Tarim: insights from igneous rocks in the Kuluketage area, NW China. Mineralogy and Petrology, 2017, 111, 237-252.	0.4	9
110	Plumeâ€orogenic lithosphere interaction recorded in the Haladala layered intrusion in the Southwest Tianshan Orogen, NW China. Journal of Geophysical Research: Solid Earth, 2016, 121, 1525-1545.	1.4	21
111	A Possible Mechanism to Thin Lithosphere of the North China Craton: Insights from Cretaceous Mafic Dikes in the Jiaodong Pensinsula. Acta Geologica Sinica, 2016, 90, 106-108.	0.8	1
112	Rapid lithospheric thinning of the North China Craton: New evidence from cretaceous mafic dikes in the Jiaodong Peninsula. Chemical Geology, 2016, 432, 1-15.	1.4	96
113	Climatic and tectonic controls on Late Triassic to Middle Jurassic sedimentation in northeastern Guangdong Province, South China. Tectonophysics, 2016, 677-678, 68-87.	0.9	9
114	High-alumina basalts from the Bogda Mountains suggest an arc setting for Chinese Northern Tianshan during the Late Carboniferous. Lithos, 2016, 256-257, 165-181.	0.6	47
115	Boron isotopes reveal multiple metasomatic events in the mantle beneath the eastern North China Craton. Geochimica Et Cosmochimica Acta, 2016, 194, 77-90.	1.6	26
116	Petrogenesis and geodynamic implications of the Late Carboniferous felsic volcanics in the Bogda belt, Chinese Northern Tianshan. Gondwana Research, 2016, 39, 165-179.	3.0	24
117	Dyke swarms: keys to paleogeographic reconstructions. Science Bulletin, 2016, 61, 1669-1671.	4.3	4
118	Coexisting Early Cretaceous High-Mg Andesites and Adakitic Rocks in the North China Craton: the Role of Water in Intraplate Magmatism and Cratonic Destruction. Journal of Petrology, 2016, 57, 1279-1308.	1.1	56
119	B isotopes of Carboniferousâ€Permian volcanic rocks in the Tuha basin mirror a transition from subduction to intraplate setting in Central Asian Orogenic Belt. Journal of Geophysical Research: Solid Earth, 2016, 121, 7946-7964.	1.4	18
120	High-Mg adakitic rocks and their complementary cumulates formed by crystal fractionation of hydrous mafic magmas in a continental crustal magma chamber. Lithos, 2016, 260, 211-224.	0.6	17
121	Origin of high-An plagioclase in the early Permian (~280 Ma) Xiaohaizi wehrlite, Northwest China: insights from melt inclusions in clinopyroxene macrocrysts and zircon oxygen isotopes. International Geology Review, 2016, 58, 1005-1019.	1.1	5
122	Petrogenesis and geochemistry of the Late Carboniferous rear-arc (or back-arc) pillow basaltic lava in the Bogda Mountains, Chinese North Tianshan. Lithos, 2016, 244, 30-42.	0.6	53
123	Clarifying the distal to proximal tephrochronology of the Millennium (B–Tm) eruption, Changbaishan Volcano, northeast China. Quaternary Geochronology, 2016, 33, 61-75.	0.6	45
124	Lateral variation in oxygen fugacity and halogen contents in early Cretaceous magmas in Jiaodong area, East China: Implication for triggers of the destruction of the North China Craton. Lithos, 2016, 248-251, 478-492.	0.6	16
125	Olivine and melt inclusion chemical constraints on the source of intracontinental basalts from the eastern North China Craton: Discrimination of contributions from the subducted Pacific slab. Geochimica Et Cosmochimica Acta, 2016, 178, 1-19.	1.6	68
126	Re-evaluating the geochronology of the Permian Tarim magmatic province: implications for temporal evolution of magmatism. Journal of the Geological Society, 2016, 173, 228-239.	0.9	22

#	Article	IF	CITATIONS
127	High-resolution SIMS oxygen isotope analysis on conodont apatite from South China and implications for the end-Permian mass extinction. Palaeogeography, Palaeoclimatology, Palaeoecology, 2016, 448, 26-38.	1.0	133
128	Provenance of Cretaceous trench slope sediments from the Mesozoic Wandashan Orogen, NE China: Implications for determining ancient drainage systems and tectonics of the Paleo-Pacific. Tectonics, 2015, 34, 1269-1289.	1.3	54
129	Composition of the Tarim mantle plume: Constraints from clinopyroxene antecrysts in the early Permian Xiaohaizi dykes, NW China. Lithos, 2015, 230, 69-81.	0.6	25
130	Crustal velocity structure in the Emeishan large igneous province and evidence of the Permian mantle plume activity. Science China Earth Sciences, 2015, 58, 1133-1147.	2.3	53
131	Magma mixing origin for high Ba–Sr granitic pluton in the Bayankhongor area, central Mongolia: Response to slab roll-back. Journal of Asian Earth Sciences, 2015, 113, 353-368.	1.0	31
132	Disequilibrium-induced initial Os isotopic heterogeneity in gram aliquots of single basaltic rock powders: Implications for dating and source tracing. Chemical Geology, 2015, 406, 10-17.	1.4	27
133	Pyroxenite-derived Early Cretaceous lavas in the Liaodong Peninsula: Implication for metasomatism and thinning of the lithospheric mantle beneath North China Craton. Lithos, 2015, 227, 77-93.	0.6	30
134	Are continental "adakites―derived from thickened or foundered lower crust?. Earth and Planetary Science Letters, 2015, 419, 125-133.	1.8	176
135	The Permian Dongfanghong island-arc gabbro of the Wandashan Orogen, NE China: Implications for Paleo-Pacific subduction. Tectonophysics, 2015, 659, 122-136.	0.9	119
136	Magmatic underplating and crustal growth in the Emeishan Large Igneous Province, SW China, revealed by a passive seismic experiment. Earth and Planetary Science Letters, 2015, 432, 103-114.	1.8	78
137	Late Triassic bimodal igneous rocks in eastern Heilongjiang Province, NE China: Implications for the initiation of subduction of the Paleo-Pacific Plate beneath Eurasia. Journal of Asian Earth Sciences, 2015, 97, 406-423.	1.0	110
138	Zircon U–Pb dating, geochemistry and Sr–Nd–Pb–Hf isotopes of the Wajilitag alkali mafic dikes, and associated diorite and syenitic rocks: Implications for magmatic evolution of the Tarim large igneous province. Lithos, 2015, 212-215, 428-442.	0.6	32
139	Petrology and Sr–Nd Isotopic Disequilibrium of the Xiaohaizi Intrusion, NW China: Genesis of Layered Intrusions in the Tarim Large Igneous Province. Journal of Petrology, 2014, 55, 2567-2598.	1.1	32
140	Thinning and destruction of the cratonic lithosphere: A global perspective. Science China Earth Sciences, 2014, 57, 2878-2890.	2.3	102
141	Anticlockwise P-T evolution at â^1⁄4280Ma recorded from ultrahigh-temperature metapelitic granulite in the Chinese Altai orogenic belt, a possible link with the Tarim mantle plume?. Journal of Asian Earth Sciences, 2014, 94, 1-11.	1.0	51
142	CA-TIMS zircon U–Pb dating of felsic ignimbrite from the Binchuan section: Implications for the termination age of Emeishan large igneous province. Lithos, 2014, 204, 14-19.	0.6	183
143	Stratigraphic evolution of a Late Triassic to Early Jurassic intracontinental basin in southeastern South China: A consequence of flat-slab subduction?. Sedimentary Geology, 2014, 302, 44-63.	1.0	22
144	Origin of the early Permian Wajilitag igneous complex and associated Fe–Ti oxide mineralization in the Tarim large igneous province, NW China. Journal of Asian Earth Sciences, 2014, 84, 51-68.	1.0	36

#	Article	IF	CITATIONS
145	The Early Permian Tarim Large Igneous Province: Main characteristics and a plume incubation model. Lithos, 2014, 204, 20-35.	0.6	216
146	Recycled oceanic crust in the source of 90–40Ma basalts in North and Northeast China: Evidence, provenance and significance. Geochimica Et Cosmochimica Acta, 2014, 143, 49-67.	1.6	114
147	Two episodes of volcanism in the Wudalianchi volcanic belt, NE China: Evidence for tectonic controls on volcanic activities. Journal of Volcanology and Geothermal Research, 2014, 285, 170-179.	0.8	32
148	Plume-lithosphere interaction in the generation of the Tarim large igneous province, NW China: Geochronological and geochemical constraints. Numerische Mathematik, 2014, 314, 314-356.	0.7	120
149	Origin of two types of rhyolites in the Tarim Large Igneous Province: Consequences of incubation and melting of a mantle plume. Lithos, 2014, 204, 59-72.	0.6	49
150	Triggers of Permo-Triassic boundary mass extinction in South China: The Siberian Traps or Paleo-Tethys ignimbrite flare-up?. Lithos, 2014, 204, 258-267.	0.6	75
151	Chemical heterogeneity of the Emeishan mantle plume: Evidence from highly siderophile element abundances in picrites. Journal of Asian Earth Sciences, 2014, 79, 191-205.	1.0	14
152	Geochronology and geochemistry of Cenozoic basalts from eastern Guangdong, SE China: constraints on the lithosphere evolution beneath the northern margin of the South China Sea. Contributions To Mineralogy and Petrology, 2013, 165, 437-455.	1.2	77
153	Precise measurement of stable (l̂´88/86Sr) and radiogenic (87Sr/86Sr) strontium isotope ratios in geological standard reference materials using MC-ICP-MS. Science Bulletin, 2013, 58, 3111-3118.	1.7	45
154	Implications from zircon-saturation temperatures and lithological assemblages for Early Permian thermal anomaly in northwest China. Lithos, 2013, 182-183, 125-133.	0.6	31
155	Precise measurement of stable neodymium isotopes of geological materials by using MC-ICP-MS. Journal of Analytical Atomic Spectrometry, 2013, 28, 1926.	1.6	36
156	Provenance of sediments from Mesozoic basins in western Shandong: Implications for the evolution of the eastern North China Block. Journal of Asian Earth Sciences, 2013, 76, 12-29.	1.0	38
157	Mineralogy and geochemistry of claystones from the Guadalupian–Lopingian boundary at Penglaitan, South China: Insights into the pre-Lopingian geological events. Journal of Asian Earth Sciences, 2013, 62, 438-462.	1.0	48
158	Detrital zircons reveal no Jurassic plateau in the eastern North China Craton. Gondwana Research, 2013, 24, 622-634.	3.0	33
159	Identification of an ancient mantle reservoir and young recycled materials in the source region of a young mantle plume: Implications for potential linkages between plume and plate tectonics. Earth and Planetary Science Letters, 2013, 377-378, 248-259.	1.8	134
160	Destruction of the North China Craton Induced by Ridge Subductions. Journal of Geology, 2013, 121, 197-213.	0.7	88
161	Sulfur in olivineâ€hosted melt inclusions from the Emeishan picrites: Implications for S degassing and its impact on environment. Journal of Geophysical Research: Solid Earth, 2013, 118, 4063-4070.	1.4	30
162	Oceanic crust components in continental basalts from Shuangliao, Northeast China: Derived from the mantle transition zone?. Chemical Geology, 2012, 328, 168-184.	1.4	174

#	Article	IF	CITATIONS
163	Temporal–spatial distribution and tectonic implications of the batholiths in the Gaoligong–Tengliang–Yingjiang area, western Yunnan: Constraints from zircon U–Pb ages and Hf isotopes. Journal of Asian Earth Sciences, 2012, 53, 151-175.	1.0	170
164	Hf isotopic characteristics of the Tarim Permian large igneous province rocks of NW China: Implication for the magmatic source and evolution. Journal of Asian Earth Sciences, 2012, 49, 191-202.	1.0	57
165	Revisiting the "Irtish tectonic beltâ€: Implications for the Paleozoic tectonic evolution of the Altai orogen. Journal of Asian Earth Sciences, 2012, 52, 117-133.	1.0	84
166	Hydrothermal fluids, argon isotopes and mineralization ages of the Fankou Pb–Zn deposit in south China: Insights from sphalerite 40Ar/39Ar progressive crushing. Geochimica Et Cosmochimica Acta, 2012, 84, 369-379.	1.6	25
167	Two tales of the continental lithospheric mantle prior to the destruction of the North China Craton: Insights from Early Cretaceous mafic intrusions in western Shandong, East China. Geochimica Et Cosmochimica Acta, 2012, 96, 193-214.	1.6	86
168	U–Pb ages and Hf isotope data from detrital zircons in the Neoproterozoic sandstones of northern Jiangsu and southern Liaoning Provinces, China: Implications for the Late Precambrian evolution of the southeastern North China Craton. Precambrian Research, 2012, 216-219, 162-176.	1.2	89
169	Metasomatized lithosphere–asthenosphere interaction during slab roll-back: Evidence from Late Carboniferous gabbros in the Luotuogou area, Central Tianshan. Lithos, 2012, 155, 67-80.	0.6	54
170	Petrology, geochemistry and Re–Os isotopes of peridotite xenoliths from Yantai, Shandong Province: Evidence for Phanerozoic lithospheric mantle beneath eastern North China Craton. Lithos, 2012, 155, 256-271.	0.6	26
171	Destruction of the North China Craton. Science China Earth Sciences, 2012, 55, 1565-1587.	2.3	440
172	Opening and evolution of the South China Sea constrained by studies on volcanic rocks: Preliminary results and a research design. Science Bulletin, 2012, 57, 3150-3164.	1.7	116
173	Effects of melt percolation on the Re-Os systematics of continental mantle lithosphere: A case study of spinel peridotite xenoliths from Heilongjiang, NE China. Science China Earth Sciences, 2012, 55, 949-965.	2.3	5
174	Recycling oceanic crust for continental crustal growth: Sr–Nd–Hf isotope evidence from granitoids in the western Junggar region, NW China. Lithos, 2012, 128-131, 73-83.	0.6	85
175	Repeated modification of lithospheric mantle in the eastern North China Craton: Constraints from SHRIMP zircon U-Pb dating of dunite xenoliths in western Shandong. Science Bulletin, 2012, 57, 651-659.	1.7	16
176	Mapping lithospheric boundaries using Os isotopes of mantle xenoliths: An example from the North China Craton. Geochimica Et Cosmochimica Acta, 2011, 75, 3881-3902.	1.6	118
177	Reply to comment on â€~Paleokarst on the top of the Maokou Formation: further evidence for domal crustal uplift prior to the Emeishan flood volcanism' by Bin He, Yi-Gang Xu, Jun-Peng Guan & Yu-Ting Zhong, Lithos 119 1–9, 2010. Lithos, 2011, 125, 1009-1011.	0.6	8
178	High-precision 40Ar/39Ar age of the gas emplacement into the Songliao Basin. Geology, 2011, 39, 451-454.	2.0	29
179	Oceanic lithospheric mantle beneath the continental crust of the Chinese Altai. Journal of the Geological Society, 2011, 168, 995-1000.	0.9	14
180	Thermal state and structure of the lithosphere beneath eastern China: A synthesis on basalt-borne xenoliths. Journal of Earth Science (Wuhan, China), 2010, 21, 711-730.	1.1	42

#	Article	IF	CITATIONS
181	Wet deposition of nitrogen and sulfur in Guangzhou, a subtropical area in South China. Environmental Monitoring and Assessment, 2010, 171, 429-439.	1.3	35
182	Primitive magmas in the Emeishan Large Igneous Province, southwestern China and northern Vietnam. Lithos, 2010, 119, 75-90.	0.6	89
183	Silicic magmas from the Emeishan large igneous province, Southwest China: Petrogenesis and their link with the end-Guadalupian biological crisis. Lithos, 2010, 119, 47-60.	0.6	148
184	The Guadalupian–Lopingian boundary mudstones at Chaotian (SW China) are clastic rocks rather than acidic tuffs: Implication for a temporal coincidence between the end-Guadalupian mass extinction and the Emeishan volcanism. Lithos, 2010, 119, 10-19.	0.6	137
185	Os, Nd and Sr isotope and trace element geochemistry of the Muli picrites: Insights into the mantle source of the Emeishan Large Igneous Province. Lithos, 2010, 119, 108-122.	0.6	75
186	Post-collisional plutons in the Balikun area, East Chinese Tianshan: Evolving magmatism in response to extension and slab break-off. Lithos, 2010, 119, 269-288.	0.6	205
187	Paleokarst on the top of the Maokou Formation: Further evidence for domal crustal uplift prior to the Emeishan flood volcanism. Lithos, 2010, 119, 1-9.	0.6	64
188	Diverse Permian magmatism in the Tarim Block, NW China: Genetically linked to the Permian Tarim mantle plume?. Lithos, 2010, 119, 537-552.	0.6	156
189	Mineralogical and Geochemical Constraints on the Petrogenesis of Post-collisional Potassic and Ultrapotassic Rocks from Western Yunnan, SW China. Journal of Petrology, 2010, 51, 1617-1654.	1.1	120
190	A Permian large igneous province in Tarim and Central Asian orogenic belt, NW China: Results of a ca. 275 Ma mantle plume?. Bulletin of the Geological Society of America, 2010, 122, 2020-2040.	1.6	140
191	U–Pb and Hf isotope analyses of detrital zircons from Late Paleozoic sediments: Insights into interactions of the North China Craton with surrounding plates. Journal of Asian Earth Sciences, 2010, 39, 335-346.	1.0	82
192	Remnants of oceanic lower crust in the subcontinental lithospheric mantle: Trace element and Sr–Nd–O isotope evidence from aluminous garnet pyroxenite xenoliths from Jiaohe, Northeast China. Earth and Planetary Science Letters, 2010, 297, 413-422.	1.8	76
193	Variations of Sr–Nd–Hf isotopic systematics in basalt during intensive weathering. Chemical Geology, 2010, 269, 376-385.	1.4	44
194	Geochemistry of TTG and TTG-like gneisses from Lushan-Taihua complex in the southern North China Craton: Implications for late Archean crustal accretion. Precambrian Research, 2010, 182, 43-56.	1.2	170
195	Distribution, regional sources and deposition fluxes of organochlorine pesticides in precipitation in Guangzhou, South China. Atmospheric Research, 2010, 97, 115-123.	1.8	28
196	Magmatic diapirism of the Fangshan pluton, southwest of Beijing, China. Journal of Structural Geology, 2009, 31, 615-626.	1.0	57
197	Neoproterozoic adakitic rocks from Mopanshan in the western Yangtze Craton: Partial melts of a thickened lower crust. Lithos, 2009, 112, 367-381.	0.6	182
198	Distribution and deposition of polycyclic aromatic hydrocarbons in precipitation in Guangzhou, South China. Journal of Environmental Sciences, 2009, 21, 654-660.	3.2	25

#	Article	IF	CITATIONS
199	Activation of northern margin of the North China Craton in Late Paleozoic: Evidence from U-Pb dating and Hf isotopes of detrital zircons from the Upper Carboniferous Taiyuan Formation in the Ningwu-Jingle basin. Science Bulletin, 2009, 54, 677-686.	1.7	52
200	On the timing and duration of the destruction of the North China Craton. Science Bulletin, 2009, 54, 3379-3396.	4.3	218
201	Pre-eruptive uplift in the Emeishan?. Nature Geoscience, 2009, 2, 530-531.	5.4	20
202	Chemical composition and seasonal variation of acid deposition in Guangzhou, South China: Comparison with precipitation in other major Chinese cities. Environmental Pollution, 2009, 157, 35-41.	3.7	104
203	Hf–Nd isotopic decoupling in continental mantle lithosphere beneath Northeast China: Effects of pervasive mantle metasomatism. Journal of Asian Earth Sciences, 2009, 35, 554-570.	1.0	39
204	Late Archean to Early Proterozoic lithospheric mantle beneath the western North China craton: Sr–Nd–Os isotopes of peridotite xenoliths from Yangyuan and Fansi. Lithos, 2008, 102, 25-42.	0.6	128
205	Petrogenesis and tectonic implications of Neoproterozoic, highly fractionated A-type granites from Mianning, South China. Precambrian Research, 2008, 165, 190-204.	1.2	108
206	Detrital zircon evidence from Burma for reorganization of the eastern Himalayan river system. Numerische Mathematik, 2008, 308, 618-638.	0.7	96
207	Zircon U–Pb and Hf isotope constraints on crustal melting associated with the Emeishan mantle plume. Geochimica Et Cosmochimica Acta, 2008, 72, 3084-3104.	1.6	233
208	Eocene break-off of the Neo-Tethyan slab as inferred from intraplate-type mafic dykes in the Gaoligong orogenic belt, eastern Tibet. Chemical Geology, 2008, 255, 439-453.	1.4	137
209	Thick, high-velocity crust in the Emeishan large igneous province, southwestern China: Evidence for crustal growth by magmatic underplating or intraplating. , 2007, , 841-858.		21
210	Age and duration of the Emeishan flood volcanism, SW China: Geochemistry and SHRIMP zircon U–Pb dating of silicic ignimbrites, post-volcanic Xuanwei Formation and clay tuff at the Chaotian section. Earth and Planetary Science Letters, 2007, 255, 306-323.	1.8	369
211	Regional uplift associated with continental large igneous provinces: The roles of mantle plumes and the lithosphere. Chemical Geology, 2007, 241, 282-318.	1.4	203
212	Os, Pb, and Nd isotope geochemistry of the Permian Emeishan continental flood basalts: Insights into the source of a large igneous province. Geochimica Et Cosmochimica Acta, 2007, 71, 2104-2119.	1.6	109
213	Mobilization and re-distribution of major and trace elements during extreme weathering of basalt in Hainan Island, South China. Geochimica Et Cosmochimica Acta, 2007, 71, 3223-3237.	1.6	244
214	Late Permian Emeishan Flood Basalts in Southwestern China. Earth Science Frontiers, 2007, 14, 1-9.	0.5	22
215	Integration of geology, geophysics and geochemistry: A key to understanding the North China Craton. Lithos, 2007, 96, 1-21.	0.6	529
216	Diachronous lithospheric thinning of the North China Craton and formation of the Daxin'anling–Taihangshan gravity lineament. Lithos, 2007, 96, 281-298.	0.6	235

#	Article	IF	CITATIONS
217	Exsolution lamellae in a clinopyroxene megacryst aggregate from Cenozoic basalt, Leizhou Peninsula, South China: petrography and chemical evolution. Contributions To Mineralogy and Petrology, 2007, 154, 691-705.	1.2	60
218	Geochronologic and petrochemical evidence for the genetic link between the Maomaogou nepheline syenites and the Emeishan large igneous province. Science Bulletin, 2007, 52, 949-958.	1.7	24
219	Identification of mantle plumes in the Emeishan Large Igneous Province. Episodes, 2007, 30, 32-42.	0.8	63
220	Kinematics and 40Ar/39Ar geochronology of the Gaoligong and Chongshan shear systems, western Yunnan, China: Implications for early Oligocene tectonic extrusion of SE Asia. Tectonophysics, 2006, 418, 235-254.	0.9	154
221	Old EMI-type enriched mantle under the middle North China Craton as indicated by Sr and Nd isotopes of mantle xenoliths from Yangyuan, Hebei Province. Science Bulletin, 2006, 51, 1343-1349.	1.7	17
222	Sedimentation and Lithofacies Paleogeography in Southwestern China Before and After the Emeishan Flood Volcanism: New Insights into Surface Response to Mantle Plume Activity. Journal of Geology, 2006, 114, 117-132.	0.7	84
223	Domains and enrichment mechanism of the lithospheric mantle in western Yunnan: A comparative study on two types of Cenozoic ultrapotassic rocks. Science in China Series D: Earth Sciences, 2005, 48, 326-337.	0.9	15
224	Mafic volcaniclastic deposits in flood basalt provinces: A review. Journal of Volcanology and Geothermal Research, 2005, 145, 281-314.	0.8	136
225	Role of lithosphere–asthenosphere interaction in the genesis of Quaternary alkali and tholeiitic basalts from Datong, western North China Craton. Chemical Geology, 2005, 224, 247-271.	1.4	266
226	Contrasting Cenozoic Lithospheric Evolution and Architecture in the Western and Eastern Sinoâ€Korean Craton: Constraints from Geochemistry of Basalts and Mantle Xenoliths. Journal of Geology, 2004, 112, 593-605.	0.7	152
227	Geologic, geochemical, and geophysical consequences of plume involvement in the Emeishan flood-basalt province. Geology, 2004, 32, 917.	2.0	405
228	Contrasting Enrichments in High- and Low-Temperature Mantle Xenoliths from Nushan, Eastern China: Results of a Single Metasomatic Event during Lithospheric Accretion?. Journal of Petrology, 2004, 45, 321-341.	1.1	66
229	Early Cretaceous gabbroic complex from Yinan, Shandong Province: petrogenesis and mantle domains beneath the North China Craton. International Journal of Earth Sciences, 2004, 93, 1025-1041.	0.9	134
230	Crust-mantle interaction during the tectono-thermal reactivation of the North China Craton: constraints from SHRIMP zircon U–Pb chronology and geochemistry of Mesozoic plutons from western Shandong. Contributions To Mineralogy and Petrology, 2004, 147, 750-767.	1.2	279
231	Highly magnesian olivines and green-core clinopyroxenes in ultrapotassic lavas from western Yunnan, China: evidence for a complex hybrid origin. European Journal of Mineralogy, 2004, 15, 965-975.	0.4	25
232	Distinct mantle sources of low-Ti and high-Ti basalts from the western Emeishan large igneous province, SW China: implications for plume–lithosphere interaction. Earth and Planetary Science Letters, 2004, 228, 525-546.	1.8	439
233	Geochronology, petrology and geochemistry of the granulite xenoliths from Nushan, east China. Geochimica Et Cosmochimica Acta, 2004, 68, 127-149.	1.6	134
234	Origin of two differentiation trends in the Emeishan flood basalts. Science Bulletin, 2003, 48, 390-394.	1.7	23

#	Article	IF	CITATIONS
235	Paleoproterozoic lower crust beneath Nushan in Anhui Province: Evidence from zircon SHRIMP U-Pb dating on granulite xenoliths in Cenozoic alkali basalt. Science Bulletin, 2003, 48, 1381-1385.	1.7	44
236	"Reactive―harzburgites from Huinan, NE China: products of the lithosphere-asthenosphere interaction during lithospheric thinning?. Geochimica Et Cosmochimica Acta, 2003, 67, 487-505.	1.6	111
237	Sedimentary evidence for a rapid, kilometer-scale crustal doming prior to the eruption of the Emeishan flood basalts. Earth and Planetary Science Letters, 2003, 213, 391-405.	1.8	430
238	Chemostratigraphic Correlation of Upper Permian Lavas from Yunnan Province, China: Extent of the Emeishan Large Igneous Province. International Geology Review, 2003, 45, 753-766.	1.1	114
239	Origin of two differentiation trends in the Emeishan flood ba-salts. Science Bulletin, 2003, 48, 390.	1.7	5
240	Evidence for crustal components in the mantle and constraints on crustal recycling mechanisms: pyroxenite xenoliths from Hannuoba, North China. Chemical Geology, 2002, 182, 301-322.	1.4	172
241	Xenolith evidence for polybaric melting and stratification of the upper mantle beneath South China. Journal of Asian Earth Sciences, 2002, 20, 937-954.	1.0	68
242	Thermo-tectonic destruction of the archaean lithospheric keel beneath the sino-korean craton in china: evidence, timing and mechanism. Physics and Chemistry of the Earth, 2001, 26, 747-757.	0.6	747
243	Petrologic and geochemical constraints on the petrogenesis of Permian–Triassic Emeishan flood basalts in southwestern China. Lithos, 2001, 58, 145-168.	0.6	785
244	Exotic lithosphere mantle beneath the western Yangtze craton: Petrogenetic links to Tibet using highly magnesian ultrapotassic rocks. Geology, 2001, 29, 863.	2.0	113
245	Distribution of trace elements in spinel and garnet peridotites. Science in China Series D: Earth Sciences, 2000, 43, 166-175.	0.9	10
246	Trace element characteristics and origin of intergranular components in mantle peridotites. Science Bulletin, 2000, 45, 643-649.	1.7	4
247	The geotherm of the lithosphere beneath Qilin, SE China: a re-appraisal and implications for P–T estimation of Fe-rich pyroxenites. Lithos, 1999, 47, 181-193.	0.6	21
248	Melt percolation and reaction atop a plume: evidence from the poikiloblastic peridotite xenoliths from Borée (Massif Central, France). Contributions To Mineralogy and Petrology, 1998, 132, 65-84.	1.2	76
249	Relation between texture and chemical composition of peridotite xenoliths and its implications: An example from Wangqing Jilin Province. Science Bulletin, 1998, 43, 837-840.	1.7	0
250	Fractionation of platinum group elements in upper mantle: Evidence from peridotite xenoliths from Wangqing. Science in China Series D: Earth Sciences, 1998, 41, 354-361.	0.9	8
251	Geodynamics of the North China Craton. Geodynamic Series, 1998, , 155-165.	0.1	175
252	Amphibole-bearing peridotite xenoliths from Nushan, Anhui Province: Evidence for melt percolation process in the upper mantle and lithospheric uplift. Diqiu Huaxue, 1997, 16, 213-229.	0.5	9

#	Article	IF	CITATIONS
253	K-rich glass-bearing wehrlite xenoliths from Yitong, Northeastern China: petrological and chemical evidence for mantle metasomatism. Contributions To Mineralogy and Petrology, 1996, 125, 406-420.	1.2	64
254	The upper mantle beneath the continental rift of Tanlu, Eastern China: evidence for the intra-lithospheric shear zones. Tectonophysics, 1993, 225, 337-360.	0.9	46